The Journal of Experimental Biology 207, 683-696
Published by The Company of Biologists 2004
doi:10.1242/jeb.00812

The dichotomous oxyregulatory behaviour of the planktonic crustacean *Daphnia magna*

R. Pirow* and I. Buchen

Institut für Zoophysiologie, Westfälische Wilhelms-Universität, Hindenburgplatz 55, 48143 Münster, Germany

*Author for correspondence (e-mail: pirow@uni-muenster.de)

Accepted 24 November 2003

Summary

The dual function of appendage movement (food acquisition, ventilation) proved to be the key to explaining the peculiar oxyregulatory repertoire of the planktonic filter feeder *Daphnia magna*. Short-term hypoxic exposure experiments with normoxia-acclimated animals under varying food concentrations revealed a dichotomous response pattern with a compensatory tachycardia under food-free conditions and a ventilatory compensation prevailing under food-rich conditions. Food-free, normoxic conditions resulted in maximum appendage beating rates (f_A) and half-maximum heart rates (f_H), which restricted the scope for oxyregulation to the circulatory system. Food-rich conditions (10^5 algal cells ml^{-1}), on the contrary, had a depressing effect on f_A whereas f_H increased to 83% of the maximum. In this physiological state, *D. magna* was able to respond to progressive hypoxia with a compensatory increase in ventilation. A conceptual and mathematical model was developed to analyse the efficiency of ventilatory and circulatory adjustments in improving oxygen transport to tissue. Model predictions showed that an increase in perfusion rate was most effective under both food-free and food-rich conditions in reducing the critical ambient oxygen tension (P_{O_2crit}) at which oxygen supply to the tissue started to become impeded. By contrast, a hypothetical increase in ventilation rate had almost no effect on P_{O_2crit} under food-free conditions, indicating that appendage movement is driven by nutritive rather than respiratory requirements. However, the model predicted a moderate reduction of P_{O_2crit} by hyperventilation under food-rich conditions. Since the regulatory scope for an adjustment in f_H was found to be limited in *D. magna* under these conditions, the increase in ventilation rate is the means of choice for a fed animal to cope with short-term, moderate reductions in ambient oxygen availability. Under long-term and more severe hypoxic conditions, however, the increase in the concentration and oxygen affinity of haemoglobin represents the one and only measure for improving the transport of oxygen from environment to cells.

Key words: Crustacea, Branchiopoda, Cladocera, *Daphnia*, zooplankton, nutrition, oxygen transport, ventilatory and circulatory system, diffusion, convection, mathematical modelling.

Introduction

To cope with fluctuations in ambient oxygen tension (P_{O_2amb}), oxyregulating water breathers must respond with appropriate adjustments of their ventilatory and circulatory systems. Systemic regulation enables these animals not only to maintain their oxygen consumption rates in the face of declining P_{O_2amb} but also to minimize the risk of oxidative stress for the tissues and to reduce the energetic expenditures for pumping medium and blood when P_{O_2amb} is high. Whether a ventilatory or a circulatory adjustment is appropriate in a given situation depends on the adjustability of the respective system, the degree of interference with other vital body functions and, perhaps most importantly, the efficiency of a ventilatory or circulatory change.

The planktonic crustacean *Daphnia magna* (Branchiopoda; Cladocera), a euryoxic species with oxyregulatory capacities (Kobayashi and Hoshi, 1984; Paul et al., 1997), exhibits a remarkable tolerance for environmental hypoxia (i.e. a state of reduced oxygen availability when the P_{O_2amb} has fallen below the normoxic values of 20–22 kPa prevailing normally at sea level; Grieshaber et al., 1994). The underlying physiological mechanisms that allow the animal to maintain oxygen uptake under environmental hypoxia range from short-term adjustments at the systemic level (Paul et al., 1997; Pirow et al., 2001) to long-term changes in the concentration and oxygen-binding characteristics of haemoglobin (Hb; Fox et al., 1951; Kobayashi and Hoshi, 1982; Kobayashi et al., 1988; Zeis et al., 2003a,b). Interestingly, the acute systemic responses to progressive, moderate hypoxia seem to deviate from those of other oxyregulating water breathers. Whereas fish (Dejours, 1981; Randall et al., 1997) or decapod crustaceans (McMahon and Wilkens, 1975; Taylor, 1976; Dejours and Beekenkamp, 1977; Herreid, 1980; Wheatly and Taylor, 1981) typically increase ventilation while keeping cardiac output (= heart rate × stroke volume) more or less constant, the situation seems to

be reversed in *D. magna*. Recent studies (Paul et al., 1997; Pirow et al., 2001) have shown that the heartbeat accelerates without notable changes in stroke volume (compensatory tachycardia) whereas the movements of the thoracic appendages, whose ventilatory function has been demonstrated experimentally (Pirow et al., 1999a), remain almost constant. It appears that hyperventilation is an inappropriate response for *D. magna* to compensate for a reduction in P_{O_2amb}.

This idea is in line with the fact that *D. magna* is able to increase the concentration of Hb in the haemolymph by more than 10 times when exposed to chronic hypoxia (Kobayashi and Hoshi, 1982). Both responses, the tachycardia and the elevation of Hb concentration, compensate for the reduction in ambient oxygen availability by increasing the oxygen transport capacity of the circulatory system (Pirow et al., 2001; Bäumer et al., 2002). This suggests that the circulatory system rather than the ventilatory system is the limiting and controlling step of the oxygen transport cascade from environment to cell. The reason for the suggested absence of a ventilatory controllability of the oxygen transport cascade could lie in the filter-feeding mode of life. The rhythmical beating of the thoracic appendages has not only a ventilatory function but also serves an important non-respiratory need: food acquisition. The third and fourth limb pairs are equipped with fine-meshed filter combs that enable *Daphnia* to retain food particles suspended in the ambient medium (Fryer, 1991). Since food particles can be highly diluted in the natural environment, the rate of medium flow required to assure an adequate nutrition could exceed the rate necessary to satisfy the oxygen demand of the animal, as is supposed for other filter feeders such as sponges, lamellibranches and ascidians (Dejours, 1981).

The dual function of appendage movement presumably provides the key to explaining the peculiar oxyregulatory behaviour of *D. magna*. However, if nutritive requirements rather than respiratory needs drive appendage movement under conditions of limited food availability, what controls this activity under excess food conditions? Several studies have shown that *Daphnia* spp. exhibits close to maximum appendage beating rates when there is little or no food available, whereas high food concentrations ($\geq 10^4$ unicellular algae ml^{-1}) effect a pronounced deceleration of appendage movement (McMahon and Rigler, 1963; Burns, 1968; Porter et al., 1982). Since the latter effect is inevitably associated with a reduction in ventilatory power, and since the oxygen demand increases as a consequence of the activation of digestive processes (Lampert, 1986; Bohrer and Lampert, 1988) despite lower energetic expenditures for appendage movement (Philippova and Postnov, 1988), it is possible that the oxyregulatory responses exhibited under these conditions deviate from those described so far (Paul et al., 1997; Pirow et al., 2001). The aim of the present paper is to analyse the oxyregulatory repertoire of *D. magna* and to provide a causal mechanistic explanation for its peculiar oxyregulatory behaviour. These issues were tackled by an experimental approach, in which the systemic responses to declining P_{O_2amb} were examined under food-free and food-rich conditions, as well as by the use of a conceptual and mathematical model, which made it possible to predict the efficiency of ventilatory and circulatory adjustments in improving oxygen transport to tissue.

Materials and methods

Animals, experimental conditions and statistical analysis

Water fleas (*Daphnia magna* Straus) were reared under normoxic conditions (80–95% air saturation, 19.5–21.5°C) as described previously (Pirow et al., 2001). Animals examined under food-free (food-deprived group) and food-rich conditions (food-provided group) had body lengths of 2.76±0.17 mm (mean ± S.D.; N=5) and 2.60±0.18 mm (N=11), respectively, with 0–8 parthenogenetic eggs or embryos in the brood chamber. The slight difference in the mean body length of both groups was not statistically significant (unpaired two-tailed t-test: t=–1.69, d.f.=14, P=0.11). The lower number of animals in the food-deprived group was regarded to be sufficient for comparative purposes since similar experiments have already been done before (Paul et al., 1997; Pirow et al., 2001).

In order to measure heart (f_H) and appendage beating rate (f_A), single animals were tethered by gluing their posterior apical spine to a 1-cm-long synthetic brush-hair with adhesive (histoacryl; B. Braun Melsungen AG, Melsungen, Germany). The animal was positioned lateral-side-down with the opposite side of the brush-hair and one of the large antennae glued onto a cover slip. The cover slip with the tethered animal was transferred into a transparent perfusion chamber (Paul et al., 1997) with the head orientated against the direction of the medium flow. The chamber was sealed and placed onto the stage of an inverted video microscope (Zeiss Axiovert 100; Carl Zeiss, Oberkochen, Germany). While keeping the animal under infrared illumination (>780 nm), the frequency of the periodic movements of the heart and the thoracic appendages were automatically determined as described in detail elsewhere (Pirow et al., 2001).

The experimental chamber was perfused with culture medium (M4; Elendt and Bias, 1990) at a flow rate of 5 ml min^{-1}. During the experiments, the oxygen tension of the medium was lowered gradually from normoxia (21 kPa) to severe hypoxia (<1.5 kPa) with a duration of five minutes for each step. This time interval was sufficient for the animal to attain a new stable level of f_H and f_A (Paul et al., 1997; Pirow et al., 2001). Different levels in oxygen tension were obtained by using two computer-driven peristaltic pumps (Gilson Minipuls 3; ABIMED, Langenfeld, Germany) that mix normoxic and anoxic media at different ratios (Freitag et al., 1998). Both media were prepared by equilibration with air or with a gas composed of 99.95% N_2 and 0.05% CO_2. The oxygen tension of the perfusion medium was measured behind the experimental chamber using a polarographic electrode (WTW Oxi 92; Weilheim, Germany). In the experiment with high food concentration, the unicellular green alga *Scenedesmus subspicatus* was added to both reservoirs at a

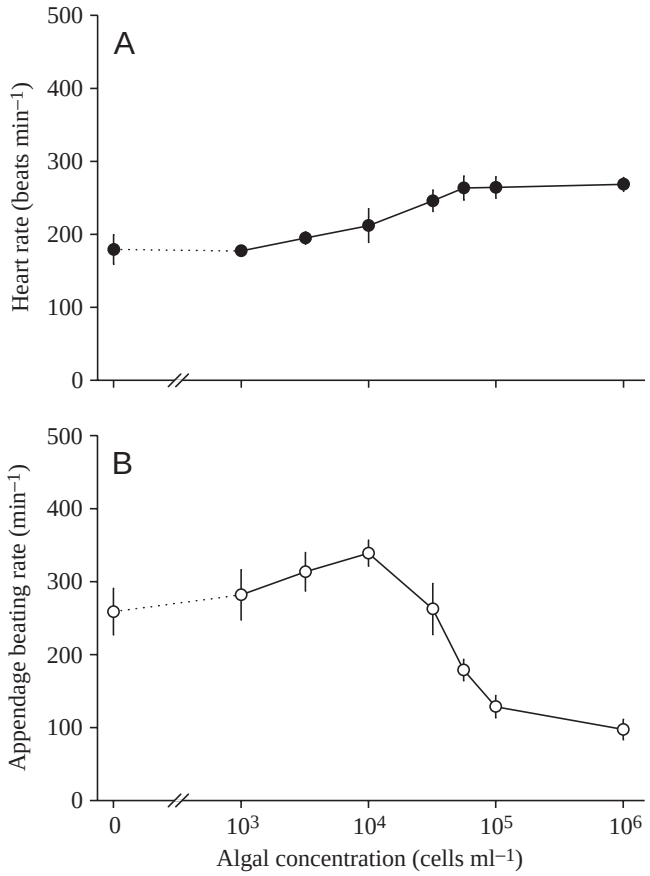

Fig. 1. Effect of increasing food concentrations on (A) appendage beating rate (f_A) and (B) heart rate (f_H) of *D. magna* (2.68±0.22 mm long) at normoxic conditions. Data are given as means ± S.D. (N=4 except for 5.6×10^4 cells ml^{-1}, where N=2). A repeated-measures ANOVA was performed for all food levels except 5.6×10^4 cells ml^{-1}. Neither the mean f_A (F=49.9, groups d.f.=6, remainder d.f.=18, P<0.001) nor the mean f_H (F=28.8, groups d.f.=6, remainder d.f.=18, P<0.001) were the same in animals on all seven food levels. The results of multiple comparisons among pairs of means are shown in Table 1.

Table 1. *Results of the Tukey multiple comparison testing among the mean appendage beating rates (f_A) and the mean heart rates (f_H) of the seven food levels*

Food level (cells ml^{-1})	Mean f_A (min^{-1})	Food level (cells ml^{-1})	Mean f_H (min^{-1})
1 000 000	97	1 000	178
100 000	129	0	179
0	259	3 200	195
32 000	262	10 000	212
1 000	282	32 000	246
3 200	313	100 000	264
10 000	339	1 000 000	269

All seven means of f_A and f_H, respectively, were arranged in order of increasing magnitude, and the vertical lines beside them represent non-significant sets of means (Sokal and Rohlf, 1995).

final concentration of 10^5 cells ml^{-1}. This concentration had been reported to effect a depression of f_A in *D. magna* (Porter et al., 1982), which was confirmed in a separate experiment (Fig. 1; Table 1). The algal stock solution was prepared by centrifuging the algae at 2000 ***g*** (5 min, 4°C) and resuspending the algal pellet in filtered culture medium (cellulose acetate filter; pore size, 0.45 μm). The concentration of algae in the stock solution was determined using a Neubauer counting chamber. The stock solution was then appropriately diluted and kept in complete darkness.

All experiments were carried out at 20°C. Animals were allowed to acclimate to the experimental conditions for 50 min before starting the experiment. f_H and f_A were analysed for the last minute of each step in oxygen tension. Data were expressed as means ± S.D., with N indicating the number of animals examined. For each experiment, in which multiple measurements were made on the same animal under various treatment levels (either food concentration or oxygen partial pressure), differences in mean values (f_H and f_A) of the different treatments levels were assessed using a repeated-measures analysis of variance (repeated-measures ANOVA; Zar, 1999). Statistical differences were considered significant at P<0.05. In the case of a statistical significant difference, multiple comparisons (Tukey test; Zar, 1999) among pairs of means using an experimentwise error rate of 0.05 were performed to determine between which means differences exist.

General description of the conceptual model of oxygen transport

Animals with a body size in the millimetre range are distinguished from their larger counterparts by short transport distances from the body surface to the central body regions. Since diffusive processes are effective for short distances only, millimetre-sized animals can rely to a greater extent on diffusion for providing peripheral tissues (i.e. tissues close to the body surface) with oxygen directly from the ventilated or non-ventilated ambient medium, whereas internal convection is, in principle, only needed to deliver oxygen to the more centrally located tissues, which are too distant from the periphery to be sufficiently supplied by diffusion. Such a pathway deviates somewhat from that of the basic vertebrate model (Taylor and Weibel, 1981; Piiper, 1982; Weibel, 1984; Shelton, 1992), where the transport of oxygen from the environment to the cells is thought to occur along a linear sequence of alternating convection and diffusion steps (ventilatory convection, diffusion across the oxygen-permeable integument, circulatory convection, diffusion in the tissue). The proposed model for the diffusive-convective oxygen transport in *Daphnia magna* incorporates both a ventilatory–circulatory transport of oxygen to the centrally located tissues as well as a diffusive supply of peripheral tissues directly from the respiratory medium (Pirow, 2003).

To keep the mathematical formulation of the oxygen transport cascade as simple as possible, the complex body shape of *D.*

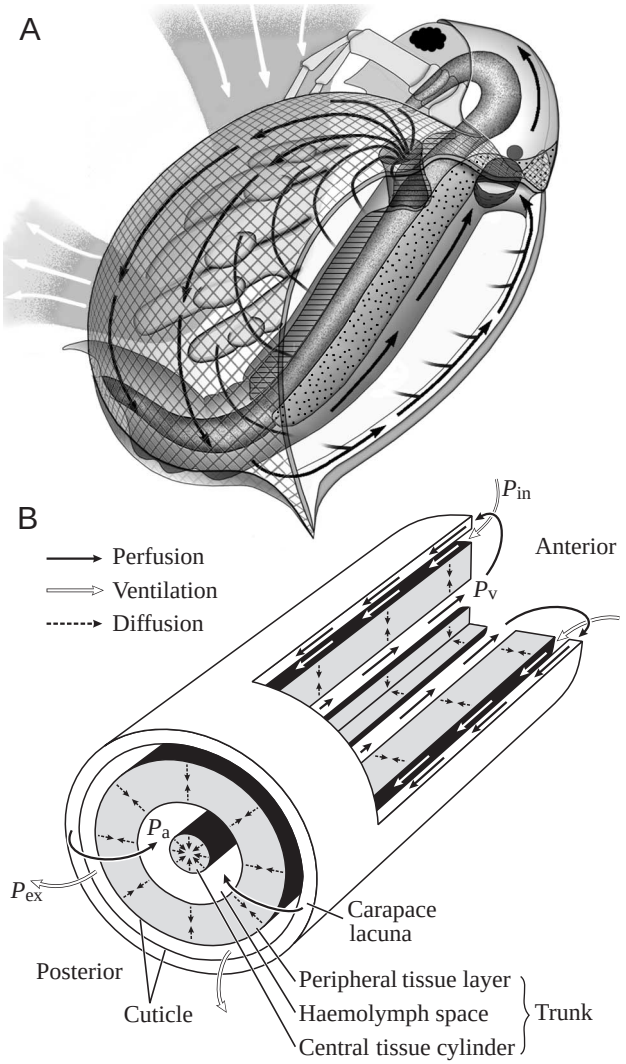

Fig. 2. (A) Dorsal view of the microcrustacean *Daphnia magna* showing the medium flow pattern (white arrows) and the circulatory pattern (black arrows). A dorsal piece of the left carapace valve (chequered area) was removed (for details see Pirow et al., 1999b). (B) Conceptual model for oxygen transport in *D. magna* based on a cylinder-within-a-tube arrangement. Medium flows through the space between the carapace and the trunk in a posterior direction (open arrows) while oxygen is released both into the carapace lacuna and the peripheral tissue layer of the trunk. This tissue layer is supplied with oxygen from the medium and from a truncal haemolymph space by diffusion (broken arrows). Oxygenated haemolymph leaves the double-walled carapace and then enters the truncal haemolymph space (solid arrows). While flowing in an anterior direction, oxygen diffuses from this haemolymph space both into the coaxial tissue cylinder and the cortical tissue layer (broken arrows). P_{in}, P_{ex}, inspiratory and expiratory oxygen partial pressures, respectively; P_a and P_v, oxygen partial pressures of the haemolymph entering and leaving the trunk, respectively.

magna (Fig. 2A) is reduced to a cylindrical trunk, which is enveloped by a hollow cylinder representing the carapace (Fig. 2B). The carapace consists of an outer and an inner wall that both enclose a haemolymph space, the carapace lacuna. The cylindrical trunk is further assumed to be composed of a peripheral tissue layer, a haemolymph space (trunk lacuna) and a central tissue cylinder (Fig. 2B). The respiratory medium flows through the space between the carapace and the trunk in a posterior direction while oxygen is released both into the carapace lacuna and the trunk. This design takes into account that the feeding current of *D. magna* is an important pathway for oxygen (Pirow et al., 1999a) and that the inner wall of the carapace is a significant site of oxygen uptake (Pirow et al., 1999b). Similar to the real situation, the medium flow and haemolymph flow in the carapace lacuna are in concurrent orientation to each other. Leaving the carapace lacuna, the oxygen-rich haemolymph enters the haemolymph space of the trunk and flows in an anterior direction while oxygen is released into both tissue compartments. Reaching the anterior position, oxygen-poor haemolymph then re-enters the carapace lacuna. The circulation of haemolymph takes place in a single circuit that, of course, is a simplification compared with the real situation, where the haemolymph flow branches into subcircuits (Pirow et al., 1999b). The oxygen partial pressure of the inspiratory and expiratory medium is denoted by P_{in} and P_{ex} (kPa), respectively, whereas that of the haemolymph entering and leaving the trunk is denoted by P_a and P_v, respectively (Fig. 2B).

Model assumptions

The following simplifying assumptions are made in the model. (1) Diffusion of oxygen in all compartments (tissue, haemolymph and medium) and across compartment interfaces is only in a radial direction. Axial diffusion is ignored in order to reduce mathematical complexity. (2) Oxygen diffusion across the tissue–medium and medium–haemolymph interfaces is impeded by cuticular barriers of the same permeability. (3) The outer wall of the carapace is assumed to be impermeable to oxygen. (4) Axial convection occurs only in the haemolymph and medium compartments. (5) Convective flows have velocity profiles that are uniform in respect to the radial axis. (6) The mixing of haemolymph leaving the lacunae at the bases of the cylindrical model as well as the re-entrance of the mixed haemolymph into destined lacunae is assumed to occur without a time delay. (7) Haemoglobin as the oxygen carrier in the haemolymph is not considered in order to reduce mathematical complexity. (8) The volume-specific oxygen consumption rate is assumed to be constant throughout the tissue compartments.

Mathematical formulation and derivation of the numerical solution

Based on assumptions made in the previous section, the following general oxygen transport equation (Groebe and Thews, 1992) accounts for radial diffusion with axial convection and oxygen consumption:

$$\underbrace{\alpha\frac{\partial P}{\partial t}}_{\substack{\text{Change}\\ \text{in } [O_2]}} = \underbrace{D\alpha\left(\frac{\partial^2 P}{\partial r^2}+\frac{1}{r}\frac{\partial P}{\partial r}\right)}_{\text{Radial diffusive } O_2 \text{ transport}} - \underbrace{v\alpha\frac{\partial P}{\partial h}}_{\substack{\text{Axial convective}\\ O_2 \text{ transport}}} - \underbrace{a}_{O_2 \text{ consumption}}. \qquad (1)$$

This equation derives from Fick's second law of diffusion

(Crank, 1975), extended by two terms for convective oxygen transport and oxygen consumption. P (kPa) is the oxygen partial pressure, t (s) and r (mm) are the time and the radial coordinate, respectively, α (nmol mm^{-3} kPa^{-1}) is the solubility coefficient for oxygen, and a (nmol s^{-1} mm^{-3}) represents the volume-specific oxygen consumption rate of pure tissue. D (mm^2 s^{-1}) is the diffusion coefficient for oxygen whereas h (mm) and v (mm s^{-1}) represent the axial coordinate and the convective velocity, respectively.

The solution of the partial differential equation 1 is approximated by numerical methods, which requires dividing the whole cylindrical body into discrete volume elements. The cylindrical model of height (h_0) and radius (r_0) is divided in the axial direction in N_{ax} equal intervals of length Δh and in the radial direction in N_{rad}+1 intervals of length Δr and $0.5\Delta r$, respectively (Fig. 3). This subdivision yields two different kinds of coaxial volume elements: solid and hollow cylinders. As a consequence of this discretization, the radii of the compartment interfaces (e.g. tissue–haemolymph interface) have to be rounded to multiples of Δr. Since the whole cylindrical body is radially symmetrical, it is sufficient to further consider only that region of the median plane that is covered by $0\ldots h_0$ and $0\ldots r_0$ (Fig. 3). In this view, each volume element is represented by a discrete grid point. The axial and radial coordinates of the grid points are $(j+0.5)\Delta h$ and $i\Delta r$, respectively, where the indices j and i are integers with j=0, 1, …, N_{ax}–1 and i=0, 1, …, N_{rad}.

By using the Taylor's series technique (Faires and Burden, 1993; Crank, 1975) for solving Fick's second law of diffusion, the following explicit finite-difference solution of equation 1 is obtained for all grid points not coinciding with compartment interfaces and excluding the central and outermost grid points at i=0 and i=N_{rad}, respectively:

$$\Delta P_{j,i} = \frac{D\Delta t}{2i(\Delta r)^2}\left[(2i+1)P_{j,i+1} - 4iP_{j,i} + (2i-1)P_{j,i-1}\right] + \frac{v\Delta t}{\Delta h}(P_{k,i} - P_{j,i}) - \frac{a\Delta t}{\alpha}. \quad (2)$$

This equation makes it possible to calculate the change in oxygen partial pressure ($\Delta P_{j,i}$) at the grid point referenced by j, i during the time interval Δt. $P_{j,i}$ represents the oxygen partial pressure at the representative grid point at time point t. The respective oxygen partial pressures of the neighbouring points at the radially inferior and superior positions are $P_{j,i-1}$ and $P_{j,i+1}$ (Fig. 3). $P_{k,i}$, relevant only in the case of axially directed convection, represents the oxygen partial pressure of the neighbouring point at the upstream position. The oxygen partial pressure of the downstream neighbouring point does not enter the convection term, because there is no gradient in the axial direction within the volume elements (axial diffusion is ignored). For grid points at the bases of the cylindrical model (at j=0 and j=N_{ax}–1), $P_{k,i}$ is appropriately replaced by P_{in}, P_a or P_v.

From the general solution given in equation 2, three special cases may be easily derived to describe the oxygen transport in the tissue compartments (D=D_T, v=0, α=α_T), in the haemolymph compartments (D=D_H, v=v_{HT} or v=v_{HC}, α=α_H, a=0) and in the medium compartment (D=D_M, v=v_M, α=α_M, a=0). In these special cases, the solubility and diffusion coefficients assume the specific values of the respective compartments (tissue – α_T, D_T; haemolymph – α_H, D_H; medium – α_M, D_M). Flow velocities of the haemolymph in the carapace lacuna and in the trunk lacuna are denoted by v_{HC} and v_{HT}, respectively.

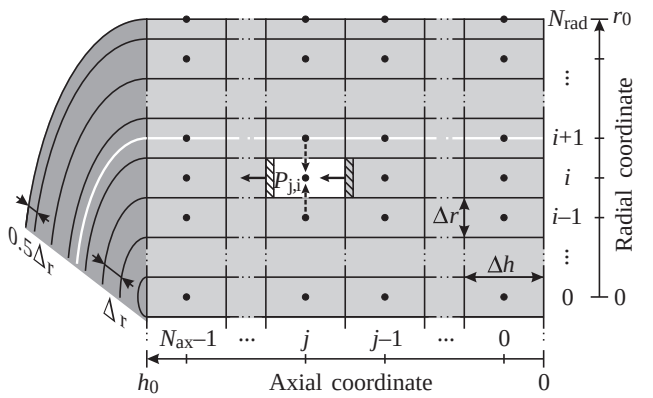

Fig. 3. Subdivision of the cylindrical model of radius r_0 and height h_0 for numerical analysis. This subdivision yields coaxial cylindrical and hollow-cylindrical volume elements of height (Δh) with radial extensions being multiples of $0.5\Delta r$. The numerical analysis aims to determine the oxygen partial pressures for the discrete set of grid points (filled circles) representing the volume elements. The axial and radial coordinates of the points are $(j+0.5)\Delta h$ and $i\Delta r$, where the indices j and i are integers with j=0, …, N_{ax}–1 and i=0, …, N_{rad}. The oxygen partial pressure ($P_{j,i}$) of a representative volume element (white rectangle) is affected by diffusive (broken arrows) and convective (solid arrows) exchange processes with the adjacent volume elements. The hatched areas represent those fractions of the respective volume elements that are shifted to the left by convection during the time interval Δt. The white line on the left exemplifies the radial position of a compartment interface that has to be rounded to a multiple of Δr.

After having derived the balance equations for the oxygen transport within the different compartments, it remains to describe the oxygen transfer across compartment interfaces as well as the changes in oxygen partial pressure at the central and outermost grid points. For the central grid points (at i=0) belonging to the tissue compartment, the following approximation is derived from Crank (1975):

$$\Delta P_{j,0} = 4\frac{D_T\Delta t}{(\Delta r)^2}(P_{j,1} - P_{j,0}) - \frac{a\Delta t}{\alpha_T}, \quad (3)$$

where $P_{j,0}$ and $P_{j,1}$ are the oxygen partial pressures at the grid points referenced by i=0 and i=1, respectively.

A somewhat more complicated mathematical formulation is required to calculate the changes in oxygen partial pressure at grid points located at compartment interfaces with an additional diffusion barrier (cuticle). In such a case, a grid point referenced by j, i is characterized by two variables, $P^u_{j,i}$ and $P^o_{j,i}$ (kPa), which represent oxygen partial pressure at the

inner and outer side of the infinitesimal thin diffusion barrier. The following example gives the specific solution for the tissue–medium interface with diffusion barrier:

$$\Delta P^{u}_{j,i} = \frac{\Delta t}{V^{u}_{i}\alpha_T}\left[\frac{B_{i-0.5}D_T\alpha_T}{\Delta r}(P_{j,i-1}-P^{u}_{j,i}) + B_i g(P^{o}_{j,i}-P^{u}_{j,i}) - V^{u}_{i}a\right], \quad (4)$$

$$\Delta P^{o}_{j,i} = \frac{\Delta t}{V^{o}_{i}\alpha_M}\left[\frac{B_{i+0.5}D_M\alpha_M}{\Delta r}(P_{j,i+1}-P^{o}_{j,i}) + B_i g(P^{u}_{j,i}-P^{o}_{j,i}) + A^{o}_{i}v_M\alpha_M(P_{j-1,i}-P^{o}_{j,i})\right]. \quad (5)$$

The parameters $B_{i-0.5}$, B_i, $B_{i+0.5}$, A^{o}_{i}, V^{u}_{i} and V^{o}_{i} are explained graphically in Fig. 4, whereas g (nmol s^{-1} mm^{-2} kPa^{-1}) represents the permeability of the cuticular diffusion barrier. The specific solution for the medium–haemolymph interface with diffusion barrier (i.e. the inner carapace wall) may be obtained by appropriately adapting equations 4 and 5.

For all compartment interfaces lacking an additional diffusion barrier, only one variable is required to describe oxygen partial pressure at that location. The following two examples show the specific solutions for the tissue–haemolymph interface (equation 6) and the outermost grid points (at $i=N_{rad}$; equation 7):

$$\Delta P_{j,i} = \frac{\Delta t}{V^{u}_{i}\alpha_T + V^{o}_{i}\alpha_H}\left[\frac{B_{i-0.5}D_T\alpha_T}{\Delta r}(P_{j,i-1}-P_{j,i}) + \frac{B_{i+0.5}D_H\alpha_H}{\Delta r}(P_{j,i+1}-P_{j,i}) + A^{o}_{i}v_{HT}\alpha_H(P_{j+1,i}-P_{j,i}) - V^{u}_{i}a\right], \quad (6)$$

$$\Delta P_{j,N_{rad}} = \frac{\Delta t}{V^{u}_{N_{rad}}}\left[\frac{B_{N_{rad}-0.5}D_H}{\Delta r}(P_{j,N_{rad}-1}-P_{j,N_{rad}}) + A^{u}_{N_{rad}}v_{HC}(P_{j-1,N_{rad}}-P_{j,N_{rad}})\right]. \quad (7)$$

The balance equations derived for all grid points were used to calculate (1) the oxygen partial pressure distribution within the model and (2) the total oxygen consumption rate as a function of P_{O_2amb}. Solutions were obtained by initially setting the oxygen partial pressure of all grid points to zero and P_{in} to P_{O_2amb}. The numerical calculation was started and continued until quasi steady-state conditions ($\Delta P_{i,j}<10^{-6}$ kPa for all grid points) were reached. For Δt, a value equal to or smaller than 0.005 s was chosen, which proved to be adequate to allow the model system to approach steady-state conditions.

Selection of parameter values

The selection of reasonable parameter values determining

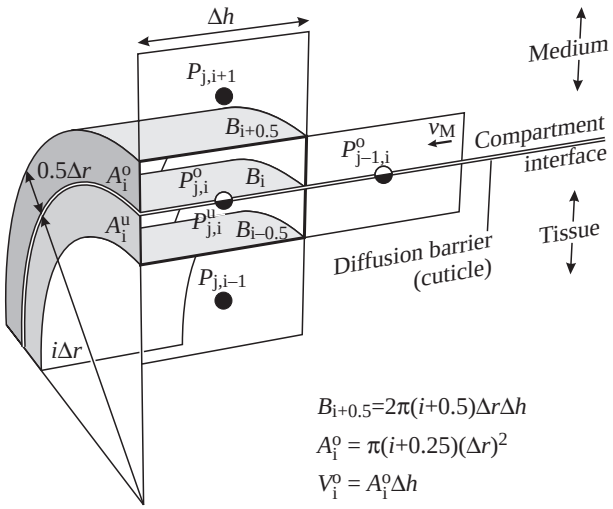

Fig. 4. Oxygen transfer across a compartment interface with additional diffusion barrier (cuticle). The grid point referenced by the indices i and j is located on an infinitesimal thin diffusion barrier separating the tissue from the medium compartment. This grid point is characterized by two variables, $P^{u}_{j,i}$ and $P^{o}_{j,i}$, which represent the oxygen partial pressure at the inner and the outer side of the circular diffusion barrier, respectively. To calculate the temporal changes in $P^{u}_{j,i}$ and $P^{o}_{j,i}$ (see equations 4, 5), the following geometrical parameters are required: the cylindrical wall areas $B_{i-0.5}$, B_i and $B_{i+0.5}$, the areas of the hollow-cylindrical bases A^{u}_{i} and A^{o}_{i}, and the hollow-cylindrical volumes V^{u}_{i} and V^{o}_{i}. Three example equations for calculating these parameters are given. v_M, flow velocity in the medium compartment; $P_{j,i-1}$, $P_{j,i+1}$, $P^{o}_{j-1,i}$, oxygen partial pressures of the neighbouring grid points; Δh and Δr, distance between two grid points in axial and radial direction.

the geometrical extensions and functional properties of the model is a tricky step in the modelling process, especially when parameter values are not precisely known or when the geometrical model deviates in some respects from structural or physical reality. Since model parameters can depend on each other, we defined key parameters from which derived parameters were calculated according to functional relationships (Table 2). Following this approach, the radial extensions of all compartments were derived taking the following assumptions into account. (1) Volume (V) and height (h_0) of the cylindrical model are 1.12 mm^3 and 2.5 mm, respectively, and refer to a 2.5 mm-long *D. magna* with no brood in the brood chamber (Kobayashi, 1983). (2) V comprises the tissue and haemolymph compartments. (3) The tissue fraction φ of V is 0.4 (Kobayashi, 1983). (4) The flow cross-sectional area (A_M) penetrated perpendicularly by the medium flow is 0.4 mm^2. (5) The thickness (Δx) of the carapace lacuna is 0.02 mm. (6) The fraction of total tissue (ξ) allocated to the central tissue cylinder is 0.25. (7) The radial distance (Δr) between two grid points is 0.005 mm.

Whereas the first three assumptions are easy to comprehend, points 4–7 require a brief justification. The value for A_M was derived from an experimental study (Pirow et al., 1999a; value not explicitly stated there). The value for Δx

Table 2. *Values and units of parameters used in the model*

Symbol	Value	Unit	Description
Key (primary) parameters			
V	1.12	mm^3	Body volume (haemolymph and tissue compartments)
h_0	2.5	mm	Height of the cylindrical model
A_M	0.4	mm^2	Flow cross-sectional area of the medium flow
Δx	0.02	mm	Thickness of the carapace lacuna
φ	0.4		Tissue fraction of body volume
ζ	0.25		Fraction of total tissue in the central tissue cylinder
a_0	0.0058	nmol s^{-1} mm^{-3}	Volume-specific O_2 consumption rate (whole body)
$\dot{V}_M$	0.8333	mm^3 s^{-1}	Medium flow rate
$\dot{Q}_H$	0.0311	mm^3 s^{-1}	Perfusion rate
α_M	0.0137	nmol mm^{-3} kPa^{-1}	Solubility coefficient for O_2 in water
α_H	0.0123	nmol mm^{-3} kPa^{-1}	Solubility coefficient for O_2 in haemolymph
α_T	0.0147	nmol mm^{-3} kPa^{-1}	Solubility coefficient for O_2 in tissue
D_M	0.0020	mm^2 s^{-1}	Diffusion coefficient for O_2 in water
D_H	0.0015	mm^2 s^{-1}	Diffusion coefficient for O_2 in haemolymph
D_T	0.0010	mm^2 s^{-1}	Diffusion coefficient for O_2 in tissue
g	0.0010	nmol s^{-1} mm^{-2} kPa^{-1}	Permeability of the cuticular diffusion barrier
Δr	0.005	mm	Radial distance between two grid points
Δh	0.1	mm	Axial distance between two grid points
Δt	≤0.005	s	Time interval for numerical calculation
Derived (secondary) parameters			
	0.120	mm	Radius of the central tissue cylinder
	0.280	mm	Outer radius of the truncal haemolymph space
	0.350	mm	Outer radius of the peripheral tissue layer
	0.500	mm	Outer radius of the medium lacuna
r_0	0.520	mm	Outer radius of the carapace lacuna
a	0.015	nmol s^{-1} mm^{-3}	Volume-specific O_2 consumption rate (pure tissue)
v_M	2.09	mm s^{-1}	Flow velocity of the medium in the medium lacuna
v_{HC}	0.13	mm s^{-1}	Flow velocity of the haemolymph in the carapace lacuna
v_{HT}	0.96	mm s^{-1}	Flow velocity of the haemolymph in the trunk lacuna

Data refer to a 2.5 mm-long, fasting *D. magna* without embryos in the brood chamber at food-free, normoxic conditions and to 20°C.

represents a rough estimate since the thickness of the haemolymph space varies across the carapace (Dahm, 1977; Schultz and Kennedy, 1977; Fryer, 1991). The value of 0.25 assigned to ξ is exactly that fraction of a solid cylinder that is encircled by half of the cylinder radius. This choice ensured that there is a sufficiently great sink for oxygen in the central region of the model as would be the case if haemolymph and tissue were more homogeneously distributed within the trunk. The value for Δr was chosen to divide the thin hemolymph compartment of the carapace lacuna into four intervals. The influence of these somewhat arbitrarily chosen parameter values on model behaviour is assessed by a sensitivity analysis in the Results.

The remaining parameters describing the functional properties of the model refer to 20°C and a 2.5 mm-long animal in the fasting state. The convective flow velocities (v_M, v_{HC}, v_{HT}) were derived by dividing the medium flow rate $\dot{V}_M$ (mm^3 s^{-1}) or the perfusion rate $\dot{Q}_H$ (mm^3 s^{-1}) by the respective flow cross-sectional area (Rouse, 1978; e.g. $v_M=\dot{V}_M/A_M$). $\dot{V}_M$ was calculated from f_A (360 min^{-1}; present study) according to functional relationships (Pirow et al., 1999a), whereas $\dot{Q}_H$ was obtained from stroke volume (Bäumer et al., 2002) and f_H (257 min^{-1}; present study).

The solubility of oxygen in water (α_M) was obtained from Gnaiger and Forstner (1983), taking the salinity of 0.2‰ of the culture medium into account. The solubility of oxygen in haemolymph (α_H) was assumed to be that of human plasma (58–85 g protein l^{-1}; Christophorides et al., 1969). Values reported for the oxygen solubility in tissue (α_T) vary in the range of 0.0097–0.0169 nmol mm^{-3} kPa^{-1} (Grote, 1967; Grote and Thews, 1962; Mahler et al., 1985; Thews, 1960). For the present model, a value of 0.0147 nmol mm^{-3} kPa^{-1} was chosen for the tissue compartment.

Values reported for the diffusion coefficient for oxygen in water (D_M) vary in the range of 0.0017–0.0025 mm^2 s^{-1} (Bartels, 1971; Gertz and Loeschke, 1954; Goldstick and Fatt, 1970; Grote, 1967; Grote and Thews, 1962; Hayduk and Laudie, 1974; Himmelblau, 1964; St-Denis and Fell, 1971). For the present model, a value of 0.0020 mm^2 s^{-1} was chosen. A variety of data also exist for the diffusion coefficient for oxygen in tissue (D_T; corrected to 20°C if necessary), such as 0.0008–0.0020 mm^2 s^{-1} for vertebrate skeletal or heart

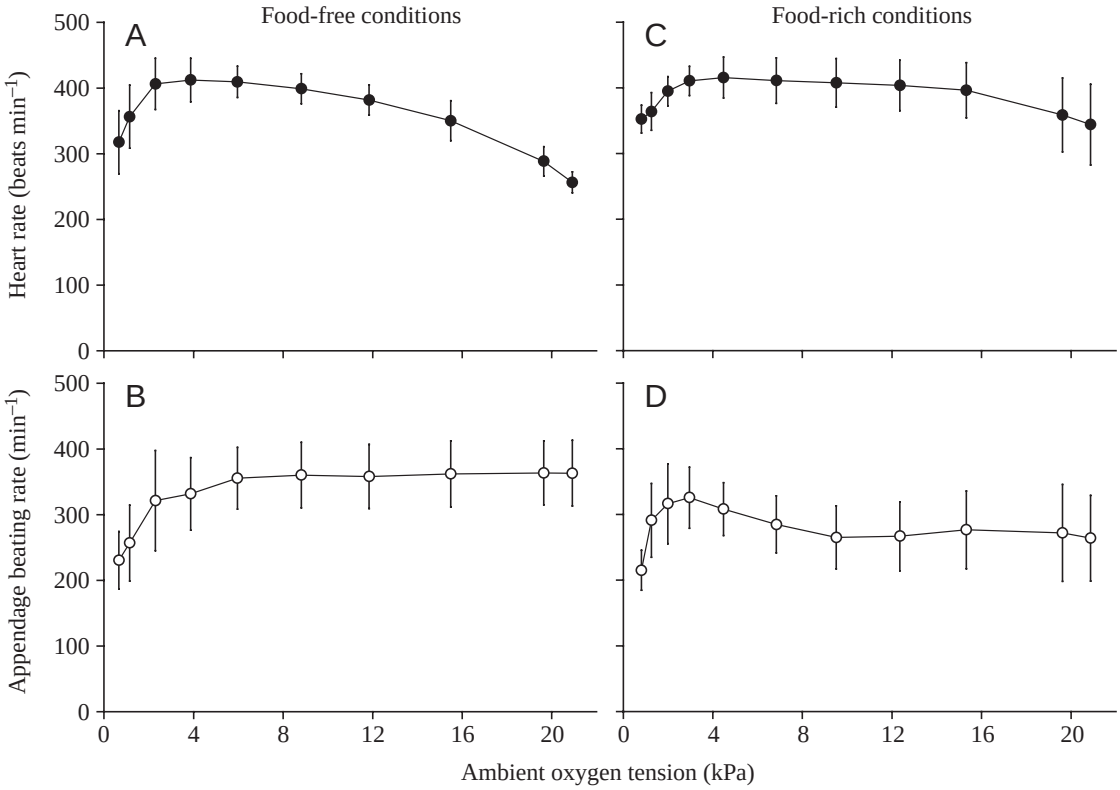

Fig. 5. Responses in (A,C) heart rate (f_H) and (B,D) appendage beating rate (f_A) to decreasing ambient oxygen tensions at food-free conditions (left; N=5) and food-rich conditions (right; 10^5 algal cells ml^{-1}; N=11 except for 0.8 kPa, where N=4). Data are given as means ± S.D. A repeated-measures ANOVA was performed for all data. At food-free conditions, the mean f_A (F=25.6, groups d.f.=9, remainder d.f.=36, P<0.001) and the mean f_H (F=48.0, groups d.f.=6, remainder d.f.=36, P<0.001) were not the same in animals on all 10 oxygen levels. At food-rich conditions, the mean f_A (F=3.1, groups d.f.=9, remainder d.f.=36, P=0.025) and the mean f_H (F=15.4, groups d.f.=9, remainder d.f.=36, P<0.001) were not the same in animals on all 10 oxygen levels. The results of multiple comparisons among pairs of means are shown in Tables 3, 4.

muscle tissue (Bentley et al., 1993; Ellsworth and Pittman, 1984; Grote and Thews, 1962; Homer et al., 1984; Mahler et al., 1985), 0.0015 mm^2 s^{-1} for rat lung tissue (Grote, 1967) and 0.0012 mm^2 s^{-1} for rat grey matter (Thews, 1960). For the present model, a value of 0.0010 mm^2 s^{-1} was chosen for the tissue compartment. For haemolymph, we assumed a diffusion coefficient to be 75% of that in water, because similar relationships (70–85%) were reported for both bovine serum (Gertz and Loeschke, 1954; Yoshida and Ohshima, 1966) and an 8.5% solution of bovine serum albumin (Kreuzer, 1950). The permeability of the cuticular diffusion barrier (g) was calculated by dividing Krogh's diffusion coefficient for oxygen in chitin (1.27×10^{-6} nmol s^{-1} cm^{-1} torr^{-1}; Krogh, 1919) by the thickness of the cuticle, for which a value of 0.001 mm was assumed (Pirow et al., 1999b).

The volume-specific oxygen consumption rate of pure tissue (a) was derived by dividing the volume-specific oxygen consumption rate of the whole animal (a_0) by the tissue fraction of body volume (φ). The value for a_0 was obtained by dividing the respiration rate (Y) of 23.6 nmol O_2 animal^{-1} h^{-1} by body volume (V). Y was calculated according to the allometric equation Y=0.3087$X^{0.95}$ (Glazier, 1991) using a dry body mass (X) of 96 μg for a 2.5 mm-long *D. magna* with no brood in the brood chamber (Kobayashi, 1983).

Results

Circulatory and ventilatory responses to hypoxia

Exposing normoxia-acclimated *D. magna* to food-free conditions with a gradual decline in ambient oxygen tension (P_{O_2amb}) resulted in a statistically significant increase in heart rate (f_H) from 257±16 min^{-1} (N=5) at normoxia (20.9 kPa) to a maximum of 412±33 min^{-1} at 3.9 kPa, followed by a deceleration of heart beat below 2.3 kPa (Fig. 5A; Table 3). Appendage beating rate (f_A) remained constant at a high level of 321–364 min^{-1} in the range of P_{O_2amb} from 20.9 kPa to 2.3 kPa but decreased significantly with a further reduction in P_{O_2amb} (Fig. 5B; Table 3).

At high food concentration (10^5 algal cells ml^{-1}), progressive hypoxia induced responses in f_H and f_A that deviated from those observed under food-free conditions. During the initial normoxic conditions, food-provided animals had a higher f_H (344±62, N=11; Fig. 5C) than those without food (257±16, N=5). In response to the progressive reduction in P_{O_2amb}, animals of both groups developed a tachycardia that

Table 3. *Results of multiple comparisons (Tukey test) among the mean appendage beating rates (*f_A*) and the mean heart rates (*f_H*) of the ten oxygen tensions (*P_{O_2amb}*) at food-free conditions*

P_{O_2amb} (kPa)	Mean f_A (min^{-1})	P_{O_2amb} (kPa)	Mean f_H (min^{-1})
0.7	230	20.9	257
1.1	258	19.6	289
2.3	321	0.7	318
3.9	332	15.5	350
6.0	356	1.1	357
11.8	358	11.8	382
8.8	360	8.8	399
15.5	362	2.3	407
20.9	363	6.0	410
19.6	364	3.9	412

All 10 sample means of f_A and f_H, respectively, were arranged by order of magnitude. In the case of statistically non-significant differences between two means, a single vertical line was drawn to the right of the appropriate sample means.

Table 4. *Results of the Tukey multiple comparison testing among the mean appendage beating rates (*f_A*) and the mean heart rates (*f_H*) of the 10 oxygen tensions (*P_{O_2amb}*) at food-rich conditions (*10^5 *algal cells* ml^{-1}*)*

P_{O_2amb} (kPa)	Mean f_A (min^{-1})	P_{O_2amb} (kPa)	Mean f_H (min^{-1})
20.9	264	20.9	344
9.5	265	19.6	359
12.4	267	1.3	364
19.6	272	2.0	395
15.3	277	15.3	397
6.8	285	12.4	404
1.3	291	9.5	408
4.5	308	3.0	411
2.0	316	6.8	411
3.0	326	4.5	416

Means were ranked in ascending order. Vertical lines indicate nonsignificant sets of means.

was more pronounced in the food-deprived group. The larger scope for circulatory adjustment in the food-deprived group resulted from a lower initial f_H, because the maximum f_H at ~4 kPa was almost the same in both groups (412±33 min^{-1} *vs* 416±31 min^{-1}). The increase in the mean f_H of the food-provided group from 344 min^{-1} at normoxia (20.9 kPa) to 395–416 min^{-1} at hypoxia (15.3–2.0 kPa) was statistically significant (Table 4).

For P_{O_2amb} values higher than 8 kPa, the f_A of food-provided animals was always lower, on average by 93 min^{-1}, than that of animals without food. The depressing effect of the high food concentration on the normoxic f_A was, however, not as great as expected from the food modulation experiment (cf. Fig. 5D and Fig. 1B). As in the food-deprived group, the reduction of P_{O_2amb} had no effect on the f_A of food-provided animals in the range from 20.9 kPa to 6.8 kPa (Fig. 5D; Table 4). However, below 8 kPa, both groups showed diverging changes in mean f_A. Whereas the f_A of food-provided animals started to rise significantly from 265±48 min^{-1} at 9.5 kPa to 326±47 min^{-1} at 3.0 kPa (Table 4), that of the food-deprived group declined non-significantly from 360±50 min^{-1} at 8.8 kPa to 321±76 min^{-1} at 2.3 kPa (Table 3).

Comparing the shape of individual response curves for f_H and f_A with that of the respective mean response curves shown in Fig. 5A–D, there was always a good correspondence between individual and mean curves except for the f_A of the food-provided animals. This group showed large interindividual variations in the initial, normoxic f_A ranging from 153 min^{-1} to 356 min^{-1} and, as a consequence, nonuniform responses to declining P_{O_2amb} (Fig. 6A). All animals that had attained an initial, normoxic f_A lower than 260 min^{-1} exhibited a pronounced hypoxia-induced increase in limb beating activity whereas those with a rate higher than 300 min^{-1} were hardly able to further elevate their f_A (Fig. 6B).

Efficiency of systemic adjustments predicted by the model

To estimate the efficiency of ventilatory and circulatory adjustments in improving oxygen transport to tissue, we examined the behaviour of the conceptual model (Fig. 2B) and determined the critical ambient oxygen tension (P_{O_2crit}) at which the rate of oxygen consumption decreased to 99% of the maximum (Fig. 7A). The data that were initially entered into the model referred to a fasting 2.5 mm-long *D. magna* exposed to food-free, normoxic conditions at 20°C (Table 2). For this physiological state, the numerical evaluation yielded a P_{O_2crit} of 10.1 kPa. At this P_{O_2crit}, the oxygen partial pressure distribution in the medium lacuna and the carapace lacuna revealed an almost complete equilibration of medium and haemolymph at the posterior part of the model (Fig. 8). The depression in oxygen consumption rate resulted from the formation of an anoxic corner in the anterior part of the central tissue cylinder. The convective contribution of the circulatory system to total oxygen supply above the P_{O_2crit} was 32% (grey-shaded area in Fig. 7A). A hypothetical doubling of medium flow rate ($\dot{V}_M$) had almost no effect on the P_{O_2crit} under these conditions (Fig. 7A). The P_{O_2crit} decreased only by 0.3 kPa. By contrast, a doubling of perfusion rate ($\dot{Q}_H$) caused a pronounced reduction of P_{O_2crit} to 7.9 kPa.

To assess the efficiency of systemic adjustments for a fed animal exposed to food-rich, normoxic conditions, new parameter values characterizing this changed physiological state were entered into the model. This state is characterized by an increased metabolic rate (Lampert, 1986; Bohrer and Lampert, 1988), a reduced f_A and an elevated f_H (cf. Figs 1, 3). The volume-specific, whole-body oxygen consumption rate (a_0) was assumed to be 50% higher than that of the fasting state (see Discussion). In addition, $\dot{V}_M$ was halved and $\dot{Q}_H$ was set

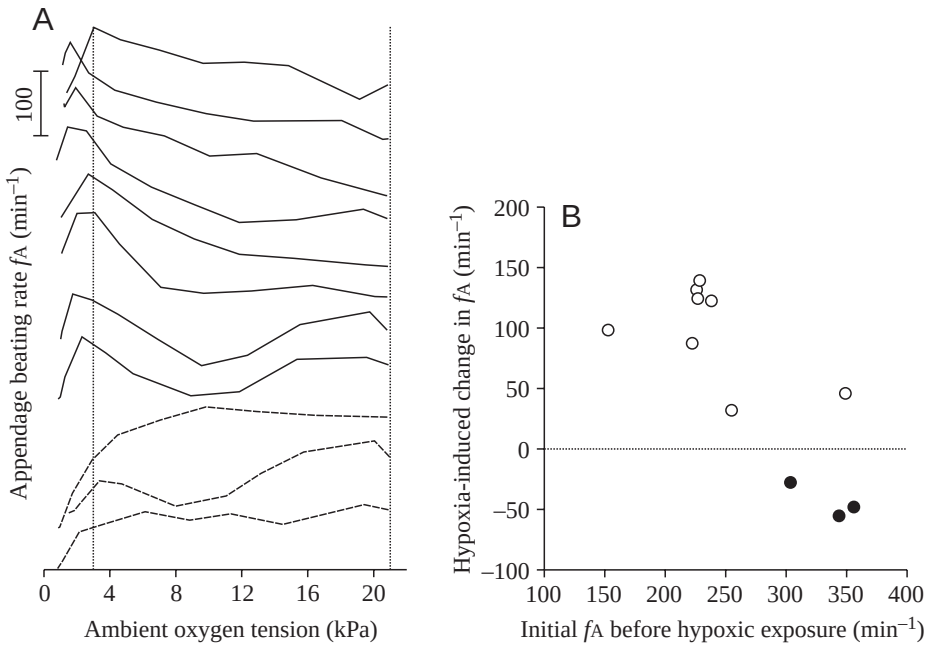

Fig. 6. (A) Individual responses (N=11) in appendage beating rate (f_A; solid and broken lines) to decreasing ambient oxygen tensions at high food concentration (10^5 algal cells ml^{-1}). The profiles were shifted vertically for clarity. Eight of 11 animals showed a hyperventilatory response (solid lines). The dotted lines indicate the two reference points, the initial normoxic level at 21 kPa and the hypoxic level of 3 kPa, which were used to assess the hypoxia-induced changes in f_A. (B) Magnitude of hypoxia-induced changes in f_A in relation to the initial f_A prevailing before the start of the hypoxic exposure. The dotted line demarcates positive (open circles) from negative responses (filled circles).

to 135% of the rate of the fasting state, thus assuming that the observed relative changes in f_A and f_H translate into the same relative changes in the respective flow rates. For this physiological state, the model yielded a P_{O_2crit} of 14.3 kPa (Fig. 7B). A doubling of $\dot{V}_M$ reduced the P_{O_2crit} by 0.7 kPa, which was more than twice as large as the decrease determined for the fasting state. Nevertheless, the change in $\dot{Q}_H$ was still most effective, because the doubling of $\dot{Q}_H$ caused a reduction of P_{O_2crit} by 3.0 kPa.

To assess the effect of changes in key parameters other than $\dot{V}_M$ and $\dot{Q}_H$, a sensitivity analysis was performed using the data from Table 2 (referring to the fasting state and food-free normoxic conditions). The value of each individual key parameter was then either decreased to 50% or increased to 200% of its initial value (all others being equal) and the percentage change in P_{O_2crit} was evaluated (Fig. 9). Of all the geometrical parameters tested (h_0, A_M, Δx, ξ), the sensitivity was highest for h_0 (height of the cylindrical model) and for ξ, which defines the allocation of tissue to the two tissue compartments. Variations in the radial and axial grid intervals (Δr, Δh) caused only minor changes (<1%) in P_{O_2crit}. The

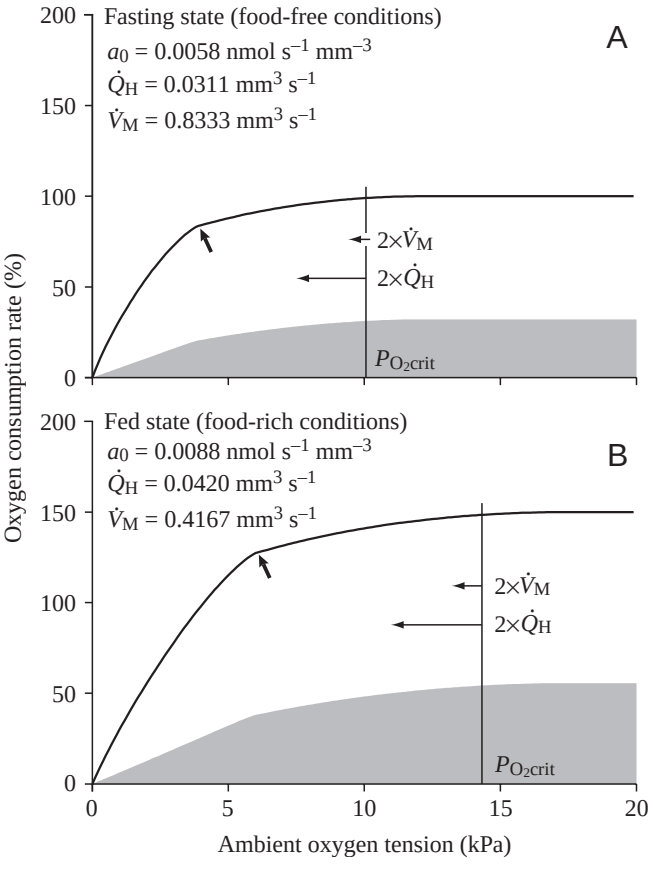

Fig. 7. Model predictions revealing the efficiency of ventilatory and circulatory adjustments. Solid curves show the predicted dependencies of the oxygen consumption rate (100%≙24 nmol h^{-1}) upon ambient oxygen tension for the fasting state/food-free conditions (A) and fed state/food-rich conditions (B). Both states differ from each other in the volume-specific oxygen consumption rate (a_0), perfusion rate ($\dot{Q}_H$) and ventilation rate ($\dot{V}_M$). $\dot{Q}_H$ and $\dot{V}_M$ represent normoxic values. Vertical lines mark the critical ambient oxygen tensions (P_{O_2crit}) at which the rates of oxygen consumption decreased to 99% of the maximum. Below P_{O_2crit}, the central tissue cylinder experiences an inadequate supply with oxygen. The overproportional decline in oxygen consumption rate in A and B below 4 kPa and 6 kPa (bold arrows), respectively, indicates the incipient impediment of oxygen provision to the peripheral tissue layer. Horizontal arrows indicate the reductions in P_{O_2crit} by hypothetically doubling either $\dot{Q}_H$ or $\dot{V}_M$. The grey shaded areas reflect the amounts of oxygen transported by the circulatory system; the remaining white areas below the solid curves are those amounts diffusing from the respiratory medium directly into the peripheral tissue layer.

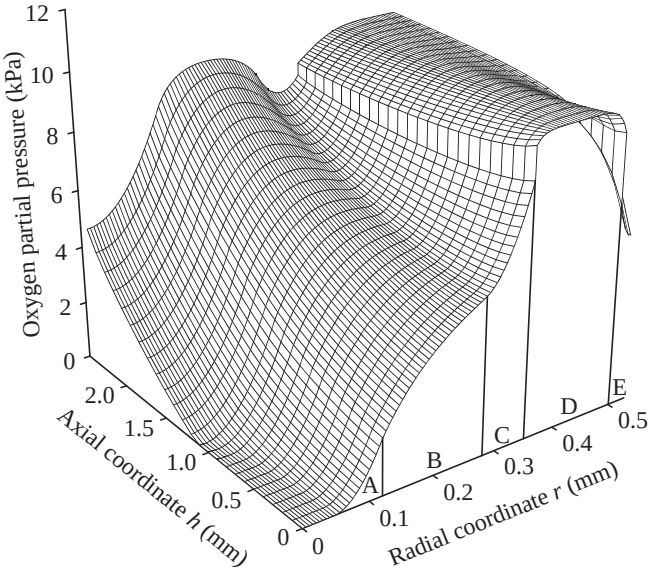

Fig. 8. Oxygen partial pressure distribution in the median plane of the radially symmetrical model at the critical ambient oxygen tension (P_{O_2crit}) of 10.1 kPa (see Fig. 7A). The upper-case letters along the radial axis mark the different compartments, and the vertical lines indicate the compartment interfaces (A, central tissue cylinder; B, truncal haemolymph space; C, peripheral tissue layer; D, medium lacuna; E, carapace lacuna). Note the formation of the anoxic corner in the central tissue cylinder.

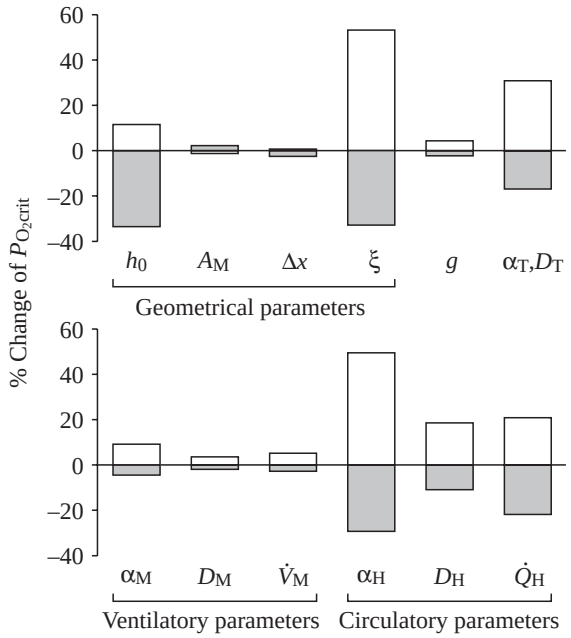

Fig. 9. Sensitivity analysis showing the effect of individual parameter changes on the critical ambient oxygen tension (P_{O_2crit}). The initial state refers to the fasting state (Table 2) with a P_{O_2crit} of 10.1 kPa (≙100%). The value of each parameter (listed by its symbol along the horizontal axis) was decreased to 50% (white) and increased to 200% (grey) of its initial value (Table 2) while keeping all other parameters unchanged.

permeability of the cuticular diffusion barrier (g) did not prove to be a limiting factor of the oxygen transport cascade, whereas changes in the diffusing properties of oxygen in tissue (α_T,D_T) had a great influence on P_{O_2crit}. Of all the parameters affecting the convective and diffusive transport of oxygen in the medium and haemolymph compartments, the solubility coefficient for oxygen in haemolymph (α_H) had the greatest impact on P_{O_2crit} (Fig. 9).

Discussion

The present study revealed that the oxyregulating species *Daphnia magna* exhibits a greater flexibility in adjusting systemic functions involved in oxygen transport than has previously been assumed (Paul et al., 1997; Pirow et al., 2001). Not only the circulatory system but also the ventilatory system proved to be sensitively tuned to ambient oxygen tension (P_{O_2amb}). The extent, however, to which the convective performance of each system could be increased during progressive hypoxia depended on the initial circulatory and ventilatory states, which in turn were largely affected by food availability and the nutritional state of the animal.

Under food-free conditions, the moderate reduction in P_{O_2amb} did not influence appendage beating rate (f_A), which was used as a measure of ventilatory performance. Heart rate (f_H), on the contrary, increased by 61%, indicating a large regulatory scope in the circulatory system under these conditions. This cardio-ventilatory response pattern was in line with the previous results (Paul et al., 1997; Pirow et al., 2001).

A reversed response pattern occurred when the animals had access to food in high concentration. Exposure to food-rich conditions (10^5 algal cells ml^{-1}) instead of food-free conditions resulted in a lower mean initial f_A (265 min^{-1} *vs* 360 min^{-1}) and a higher mean initial f_H (344 min^{-1} *vs* 257 min^{-1}). In this physiological state, with an individual f_A lower than 260 min^{-1}, *D. magna* was able to respond to a reduction in P_{O_2amb} with a compensatory increase in ventilation. The fact that four out of 11 individuals with an f_A above 300 min^{-1} failed to show this hyperventilatory response suggests that other unknown factors counteracted the depressing effect of high food concentrations on f_A. The hypoxia-induced tachycardia was less pronounced under food-rich conditions than under food-free conditions because of the higher initial f_H. These findings clearly demonstrate that the scope for a short-term improvement of oxygen transport shifted from the circulatory to the ventilatory system. The oxyregulatory repertoire of the millimetre-sized *D. magna* consequently includes a systemic response pattern that is comparable to that of large-sized, physiologically advanced water breathers such as fish (Dejours, 1981; Randall et al., 1997) or decapod crustaceans (Wheatly and Taylor, 1981).

The decelerating effect of high food concentrations on f_A has been known for quite some time (McMahon and Rigler, 1963; Burns, 1968; Porter et al., 1982). Above a critical food

concentration of 10^4 algal cells ml^{-1} (Porter et al., 1982), the amount of food retained by the filter combs of the thoracic appendages exceeds the amount that the animal is able to ingest and/or digest (Rigler, 1961). The decrease in f_A reduces the imbalance between food supply (the amount of food initially retained) and demand. However, the reduction in f_A is obviously not sufficient to remove this imbalance completely, since a higher rate of rejection movements of the postabdominal claw is required to remove superfluous food particles from the filter apparatus (Porter et al., 1982). From the energetic point of view, one would expect a further reduced or intermittent appendage activity, which would make additional rejection movements unnecessary. However, taking the dual function of appendage movement into account, it is likely that the actual f_A exhibited under these conditions represents a compromise between the need to reduce energetic expenditures for food collection and the need to satisfy the increased oxygen requirements of the fed animal.

Lampert (1986) as well as Bohrer and Lampert (1988) have shown that the respiratory rate (carbon loss per time interval) of well-fed *D. magna* is more than twice the rate of starving animals. Taking the change in the respiratory quotient from 0.7 (starved) to 1.15 (well-fed; Lampert and Bohrer, 1984) into account, this elevation in respiratory rate corresponds to a 1.4-fold increase in oxygen consumption rate. The higher oxygen demand arises from the digestion and biochemical processing of food (Bohrer and Lampert, 1988; Philippova and Postnov, 1988) and the tissues involved in this physiological task; i.e. the digestive tract and the fat cells as a storage site of reserve mass are, to a great extent, located in the central part of the trunk rather than in the peripheral body region. This is important to note because centrally located tissues are more dependent on a convective supply of oxygen *via* the circulatory system than are those in the periphery of the body, which can rely to a greater extent on a direct diffusive provision of oxygen from the ambient medium. Since the open circulatory system of *Daphnia* spp. lacks any arteries and capillaries, there is no possibility of redirecting a greater share of blood flow to these metabolically activated tissues, and an improvement of local oxygen supply can only be achieved by an increase in total perfusion rate. This could explain why the initial, normoxic f_H of food-provided animals was 34% higher than that of starving animals. Besides this explanation, a circulatory compensation for the reduction in external convection cannot be excluded. In the food-modulation experiment (Fig. 1), we observed in two of four animals a complete stop of appendage movement for 1.5 min after the food concentration had been changed from 10^6 to 0 algal cells ml^{-1}. This behavioural change, which occurred under normoxic conditions, was immediately followed by a sharp increase in f_H by 20–24%, and f_H remained at this high level until the animals resumed limb beating activity.

The experimental findings of the present study suggest that a circulatory adjustment is the most effective measure of hypoxia adaptation in the planktonic filter feeder *D. magna*, at least under low food concentrations when f_A is at a maximum. The apparent inability to further increase f_A under these conditions might result from biomechanical or energetic constraints such as the hydrodynamic resistance of the filter combs and the energetic costs of pumping medium. But even if such constraints would not exist, it is questionable whether an enhancement of ventilatory activity would have any beneficial effect, for example, in enabling the animal to sustain its rate of oxygen uptake at a far lower P_{O_2amb}. An experimental test to answer this question is hardly possible. However, since a large amount of physiological information is available for *D. magna*, this question can be approached theoretically by the use of a conceptual model.

Conceptual models have proven to be a valuable complement to experimental approaches and have made it possible to analyse, for example, the transfer characteristics and transport limitations of the different gas exchange organs of vertebrates (Piiper and Scheid, 1975). Contrary to the situation in vertebrates, the millimetre-sized *D. magna* lacks an arrangement in which the circulatory system links distinct sites for respiratory gas exchange and tissue gas transfer (Taylor and Weibel, 1981; Piiper, 1982; Weibel, 1984; Shelton, 1992). The whole integument of *D. magna* is, in principle, permeable to respiratory gases, and the oxygen is moved from the body surface to the tissues by diffusion and convection as well. We have therefore devised a conceptual model that takes a direct diffusive supply of oxygen to the peripheral tissues *via* the ambient medium and a convective supply to the centrally located tissues *via* the circulatory system into account.

The predictions made by this model gave support to the hypothesis raised in the Introduction that the circulatory system is the limiting step of the oxygen transport cascade in *D. magna*. The model analysis showed that an increase in perfusion rate was most effective both under food-free (fasting state) and food-rich (fed state) conditions in reducing the critical ambient oxygen tension (P_{O_2crit}) at which oxygen supply to the tissue started to become impeded. By contrast, an increase in ventilation rate had almost no effect on P_{O_2crit} under food-free conditions but a moderate effect under food-rich conditions. Since the regulatory scope for an adjustment in heart rate was found to be limited in *D. magna* under food-rich conditions, the increase in ventilation rate is the means of choice for a fed animal to cope with short-term, moderate hypoxia. The improvement of oxygen supply in the animal by enhancing ventilatory flow may also include the reduction of fluid and diffusive boundary layers, an aspect that was not considered in the present model. Under chronic and more severe hypoxic conditions, however, the increase in the concentration and oxygen affinity of Hb represents the one and only measure for improving the transport of oxygen from environment to cells.

In the present model, Hb was not considered as the haemolymph oxygen carrier in order to reduce mathematical complexity. This might explain why the critical ambient oxygen concentration of 3.9 mg O_2 l^{-1} (P_{O_2crit}=7.9 kPa), which was predicted for the fasting state with doubled perfusion rate (Fig. 7A), was higher than the critical oxygen concentrations of 1.3–3.0 mg O_2 l^{-1} reported for filtering and respiration rates of Hb-poor *D. magna* and *D. pulex* (Kring and O'Brien, 1976;

Heisey and Porter, 1977; Kobayashi and Hoshi, 1984). The high sensitivity of the model to changes in the solubility coefficient for oxygen in the haemolymph (α_H) indicates that Hb can have a pronounced effect on P_{O_2crit}, since it enhances both the convective and diffusive transport of oxygen in the haemolymph. The implementation of Hb-mediated oxygen transport is the next step when extending the model, which will then allow us to provide a causal mechanistic explanation for the expression of specific Hb-related characteristics (concentration, oxygen affinity, cooperativity) in animals of a given anatomical disposition and physiological constitution under different environmental conditions.

List of symbols

a	volume-specific oxygen consumption rate of pure tissue (nmol s^{-1} mm^{-3})
a_0	volume-specific oxygen consumption rate of the whole body (nmol s^{-1} mm^{-3})
A_i^u, A_i^o	area of hollow-cylindrical bases (mm^2)
A_M	flow cross-sectional area perpendicular to medium flow (mm^2)
$B_{i-0.5}$, B_i, $B_{i+0.5}$	cylindrical wall areas (mm^2)
D	diffusion coefficient for oxygen (mm^2 s^{-1})
D_H	diffusion coefficient for oxygen in haemolymph (mm^2 s^{-1})
D_M	diffusion coefficient for oxygen in medium (mm^2 s^{-1})
D_T	diffusion coefficient for oxygen in tissue (mm^2 s^{-1})
f_A	appendage beating rate (min^{-1})
f_H	heart rate (min^{-1})
g	permeability of the cuticular diffusion barrier (nmol s^{-1} mm^{-2} kPa^{-1})
h	axial coordinate (mm)
h_0	height of the cylindrical model (mm)
i, j, k	indices of grid points
N_{ax}	number of grid points in axial direction
$N_{rad}+1$	number of grid points in radial direction
P	oxygen partial pressure (kPa)
P_a	oxygen partial pressure of the haemolymph entering the trunk lacuna (kPa)
P_{ex}	oxygen partial pressure of the expiratory medium (kPa)
$P_{i,j}$	oxygen partial pressure at the grid point referenced by i, j (kPa)
$P_{j,i}^o$	oxygen partial pressure at the outer side of an infinitesimal thin diffusion barrier (kPa)
$P_{j,i}^u$	oxygen partial pressure at the inner side of an infinitesimal thin diffusion barrier (kPa)
P_{in}	oxygen partial pressure of the inspiratory medium (kPa)
P_{O_2amb}	ambient oxygen tension (kPa)
P_{O_2crit}	critical ambient oxygen tension (kPa)
P_v	oxygen partial pressure of the haemolymph leaving the trunk lacuna (kPa)
$\dot{Q}_H$	perfusion rate (mm^3 s^{-1})
r	radial coordinate (mm)
r_0	radius of the cylindrical model, outer radius of the carapace lacuna (mm)
t	time (s)
v	flow velocity (mm s^{-1})
V	volume of the cylindrical model (mm^3)
v_{HC}	flow velocity of the haemolymph in the carapace lacuna (mm s^{-1})
v_{HT}	flow velocity of the haemolymph in the trunk lacuna (mm s^{-1})
V_i^u, V_i^o	volume of hollow cylinders (mm^2)
v_M	flow velocity of the medium (mm s^{-1})
$\dot{V}_M$	medium flow rate (mm^3 s^{-1})
X	dry body mass (μg)
Y	respiration rate (nmol $animal^{-1}$ h^{-1})
Δh	distance between two grid points in axial direction (mm)
$\Delta P_{j,i}$	change in $P_{j,i}$ during Δt (kPa)
Δr	distance between two grid points in radial direction (mm)
Δt	time interval (s)
Δx	thickness of the carapace lacuna (mm)
α	solubility coefficient for oxygen (nmol mm^{-3} kPa^{-1})
α_H	solubility coefficient for oxygen in haemolymph (nmol mm^{-3} kPa^{-1})
α_M	solubility coefficient for oxygen in medium (nmol mm^{-3} kPa^{-1})
α_T	solubility coefficient for oxygen in tissue (nmol mm^{-3} kPa^{-1})
φ	tissue fraction of body volume
ξ	fraction of total tissue allocated to the central tissue cylinder

References

Bartels, H. (1971). *Biological Handbooks. Respiration and Circulation* (Table 14, p. 22). Bethesda, MD: Federation of the American Societies of Experimental Biology.

Bäumer, C., Pirow, R. and Paul, R. J. (2002). Circulatory oxygen transport in the water flea *Daphnia magna*. *J. Comp. Physiol. B* **172**, 275-285.

Bentley, T. B., Meng, H. and Pittman, R. N. (1993). Temperature dependence of oxygen diffusion and consumption in mammalian striated muscle. *Am. J. Physiol.* **264**, H1825-H1830.

Bohrer, R. N. and Lampert, W. (1988). Simultaneous measurement of the effect of food concentration on assimilation and respiration in *Daphnia magna* Straus. *Funct. Ecol.* **2**, 463-471.

Burns, C. W. (1968). Direct observations of mechanisms regulating feeding behavior of *Daphnia*, in Lakewater. *Int. Revue Ges. Hydrobiol.* **53**, 83-100.

Christophorides, C., Laasberg, L. H. and Hedley-Whyte, J. (1969). Effect of temperature on solubility of O_2 in human plasma. *J. Appl. Physiol.* **26**, 56-60.

Crank, J. (1975). *The Mathematics of Diffusion*. Oxford: Oxford University Press.

Dahm, E. (1977). Morphologische Untersuchungen an Cladoceren unter besonderer Berücksichtigung der Ultrastruktur des Carapax. *Zool. Jb. Anat.* **97**, 68-126.

Dejours, P. (1981). *Principles of Comparative Respiratory Physiology*. Amsterdam, New York, Oxford: Elsevier/North-Holland Biomedical Press.

Dejours, P. and Beekenkamp, H. (1977). Crayfish respiration as a function of water oxygenation. *Respir. Physiol.* **30**, 241-251.

Elendt, B.-P. and Bias, W.-R. (1990). Trace nutrient deficiency in *Daphnia*

magna cultured in standard medium for toxicity testing. Effects of the optimization of culture conditions on life history parameters of *D. magna*. *Wat. Res. Biol.* **24**, 1157-1167.

Ellsworth, M. L. and Pittman, R. N. (1984). Heterogeneity of oxygen diffusion through hamster striated muscles. *Am. J. Physiol.* **246**, H161-H167.

Faires, J. D. and Burden, R. L. (1993). *Numerical Methods*. Boston: PWS Publishing Company.

Fox, H. M., Gilchrist, B. M. and Phear, E. A. (1951). Functions of haemoglobin in *Daphnia*. *Proc. R. Soc. B* **138**, 514-528.

Freitag, J. F., Steeger, H.-U., Storz, U. C. and Paul, R. J. (1998). Sublethal impairment of respiratory control in plaice (*Pleuronectes platessa*) larvae induced by UV-B radiation, determined using a novel biocybernetical approach. *Mar. Biol.* **132**, 1-8.

Fryer, G. (1991). Functional morphology and the adaptive radiation of the Daphniidae (Branchiopoda: Anomopoda). *Phil. Trans. R. Soc. Lond. B* **331**, 1-99.

Gertz, K. H. and Loeschke, H. H. (1954). Bestimmung der Diffusionskoeffizienten von H_2, O_2, N_2, und He in Wasser und Blutserum bei konstant gehaltener Konvektion. *Z. Naturforsch.* **9b**, 1-9.

Glazier, D. S. (1991). Separating the respiration rates of embryos and brooding females of *Daphnia magna*: implications for the cost of brooding and the allometry of metabolic rate. *Limnol. Oceanogr.* **36**, 354-362.

Gnaiger, E. and Forstner, H. (1983). *Polarographic Oxygen Sensors*. Berlin, Heidelberg, New York: Springer Verlag.

Goldstick, T. K. and Fatt, I. (1970). Diffusion of oxygen in solutions of blood proteins. *Chem. Eng. Progr. Symp. Ser.* **66**, 101-113.

Grieshaber, M. K., Hardewig, I., Kreuzer, U. and Pörtner, H.-O. (1994). Physiological and metabolic responses to hypoxia in invertebrates. *Rev. Physiol. Pharmacol.* **125**, 63-147.

Groebe, K. and Thews, G. (1992). Basic mechanisms of diffusive and diffusion-related oxygen transport in biological systems: a review. *Adv. Exp. Med. Biol.* **317**, 21-33.

Grote, J. (1967). Die Sauerstoffdiffusionskonstanten im Lungengewebe und Wasser und ihre Temperaturabhängigkeit. *Pflügers Arch. Gesamte Physiol.* **324**, 245-254.

Grote, J. and Thews, G. (1962). Die Bedingungen für die Sauerstoffversorgung des Herzmuskelgewebes. *Pflügers Arch. Gesamte Physiol.* **276**, 142-165.

Hayduk, W. and Laudie, H. (1974). Prediction of diffusion coefficients for nonelectrolytes in dilute aqueous solutions. *Am. Inst. Chem. Eng. J.* **20**, 611-615.

Heisey, D. and Porter, K. G. (1977). The effect of ambient oxygen concentration on filtering rate and respiration rate of *Daphnia galeata mendotae* and *Daphnia magna*. *Limnol. Oceanogr.* **22**, 839-845.

Herreid, C. F. (1980). Hypoxia in invertebrates. *Comp. Biochem. Physiol. A* **67**, 311-320.

Himmelblau, D. M. (1964). Diffusion of dissolved gases in liquids. *Chem. Rev.* **64**, 527-550.

Homer, L. D., Shelton, J. B., Dorsey, C. H. and Williams, T. J. (1984). Anisotropic diffusion of oxygen in slices of rat muscle. *Am. J. Physiol.* **246**, R107-R113.

Kobayashi, M. (1983). Estimation of the haemolymph volume in *Daphnia magna* by haemoglobin determination. *Comp. Biochem. Physiol. A* **76**, 803-805.

Kobayashi, M. and Hoshi, T. (1982). Relationship between the haemoglobin concentration of *Daphnia magna* and the ambient oxygen concentration. *Comp. Biochem. Physiol. A* **72**, 247-249.

Kobayashi, M. and Hoshi, T. (1984). Analysis of respiratory role of haemoglobin in *Daphnia magna*. *Zool. Sci.* **1**, 523-532.

Kobayashi, M., Fujiki, M. and Suzuki, T. (1988). Variation in and oxygen-binding properties of *Daphnia magna* hemoglobin. *Physiol. Zool.* **61**, 415-419.

Kreuzer, F. (1950). Über die Diffusion von Sauerstoff in Serumeiweislösungen verschiedener Konzentrationen. *Helv. Physiol. Acta* **8**, 505-516.

Kring, R. L. and O'Brien, W. J. (1976). Effect of varying oxygen concentrations on the filtering rate of *Daphnia pulex*. *Ecology* **57**, 808-814.

Krogh, A. (1919). The rate of diffusion of gases through animal tissue, with some remarks on the coefficient of invasion. *J. Physiol.* **52**, 391-408.

Lampert, W. (1986). Response of the respiratory rate of *Daphnia magna* to changing food conditions. *Oecologia (Berlin)* **70**, 495-501.

Lampert, W. and Bohrer, R. (1984). Effect of food availability on the respiratory quotient of *Daphnia magna*. *Comp. Biochem. Physiol. A* **78**, 221-223.

Mahler, M., Louy, C., Homsher, E. and Peskoff, A. (1985). Reappraisal of diffusion, solubility, and consumption of oxygen in frog skeletal muscle, with application to muscle energy balance. *J. Gen. Physiol.* **86**, 105-134.

McMahon, B. and Wilkens, J. (1975). Respiratory and circulatory responses to hypoxia in the lobster *Homarus americanus*. *J. Exp. Biol.* **62**, 637-655.

McMahon, J. W. and Rigler, F. H. (1963). Mechanisms regulating the feeding rate of *Daphnia magna* Straus. *Can. J. Zool.* **41**, 321-332.

Paul, R. J., Colmorgen, M., Hüller, S., Tyroller, F. and Zinkler, D. (1997). Circulation and respiratory control in millimetre-sized animals (*Daphnia magna*, *Folsomia candida*) studied by optical methods. *J. Comp. Physiol. B* **167**, 399-408.

Philippova, T. and Postnov, A. L. (1988). The effect of food quantity on feeding and metabolic expenditure in Cladocera. *Int. Rev. Ges. Hydrobiol.* **73**, 601-615.

Piiper, J. (1982). Respiratory gas exchange at lungs, gills and tissues: mechanisms and adjustments. *J. Exp. Biol.* **100**, 5-22.

Piiper, J. and Scheid, P. (1975). Gas transport efficacy of gills, lungs and skin: theory and experimental data. *Respir. Physiol.* **23**, 209-221.

Pirow, R. (2003). The contribution of haemoglobin to oxygen transport in the microcrustacean *Daphnia magna* – a conceptual approach. *Adv. Exp. Med. Biol.* **510**, 101-107.

Pirow, R., Bäumer, C. and Paul, R. J. (2001). Benefits of haemoglobin in the cladoceran crustacean *Daphnia magna*. *J. Exp. Biol.* **204**, 3425-3441.

Pirow, R., Wollinger, F. and Paul, R. J. (1999a). Importance of the feeding current for oxygen uptake in the water flea *Daphnia magna*. *J. Exp. Biol.* **202**, 553-562.

Pirow, R., Wollinger, F. and Paul, R. J. (1999b). The sites of respiratory gas exchange in the planktonic crustacean *Daphnia magna*: an *in vivo* study employing blood haemoglobin as an internal oxygen probe. *J. Exp. Biol.* **202**, 3089-3099.

Porter, K. G., Gerritsen, J. and Orcutt, J. D. (1982). The effect of food concentration on swimming patterns, feeding behavior, assimilation, and respiration by *Daphnia*. *Limnol. Oceanogr.* **27**, 935-949.

Randall, D., Burggren, W. and French, K. (1997). *Eckert Animal Physiology: Mechanisms and Adaptations*. New York: W. H. Freeman and Company.

Rigler, F. H. (1961). The relation between the concentration of food and feeding rate of *Daphnia magna* Straus. *Can. J. Zool.* **39**, 857-868.

Rouse, H. (1978). *Elementary Mechanics of Fluids*. New York: Dover Publications, Inc.

Schultz, T. W. and Kennedy, J. R. (1977). Analyses of the integument and muscle attachment in *Daphnia pulex* (Cladocera: Crustacea). *J. Submicr. Cytol.* **9**, 37-51.

Shelton, G. (1992). Model applications in respiratory physiology. In *Oxygen Transport in Biological Systems*, vol. 51, *SEB Seminar Series* (ed. S. Egginton and H. F. Ross), pp. 1-44. Cambridge: Cambridge University Press.

Sokal, R. R. and Rohlf, F. J. (1995). *Biometry*. New York: W. H. Freeman and Company.

St-Denis, C. E. and Fell, C. J. D. (1971). Diffusivity of oxygen in water. *Can. J. Chem. Eng.* **49**, 885.

Taylor, A. (1976). The respiratory responses of *Carcinus maenas*. *J. Exp. Biol.* **65**, 309-322.

Taylor, C. R. and Weibel, E. R. (1981). Design of the mammalian respiratory system. I. Problem and strategy. *Respir. Physiol.* **44**, 1-10.

Thews, G. (1960). Ein Verfahren zur Bestimmung des O_2-Diffusionskoefficienten, der O_2-Leitfähigkeit und des O_2-Löslichkeitskoeffizienten im Gehirngewebe. *Pflügers Arch.* **271**, 227-244.

Weibel, E. R. (1984). *The Pathway for Oxygen*. Cambridge, MA: Harvard University Press.

Wheatly, M. G. and Taylor, E. W. (1981). The effect of progressive hypoxia on heart rate, ventilation, respiratory gas exchange and acid-base status in the crayfish *Austropotamobius pallipes*. *J. Exp. Biol.* **92**, 125-141.

Yoshida, F. and Ohshima, N. (1966). Diffusivity of oxygen in blood serum. *J. Appl. Physiol.* **21**, 915-919.

Zar, J. H. (1999). *Biostatistical Analysis*. Upper Saddle River, NJ: Prentice Hall.

Zeis, B., Becher, B., Goldmann, T., Clark, R., Vollmer, E., Bölke, B., Bredebusch, I., Lamkemeyer, T., Pinkhaus, O., Pirow, R. and Paul, R. J. (2003a). Differential haemoglobin gene expression in the crustacean *Daphnia magna* exposed to different oxygen partial pressures. *Biol. Chem.* **384**, 1133-1145.

Zeis, B., Becher, B., Lamkemeyer, T., Rolf, S., Pirow, R. and Paul, R. J. (2003b). The process of hypoxic induction of *Daphnia magna* hemoglobin: subunit composition and functional properties. *Comp. Biochem. Physiol. B* **134**, 243-252.